Electronic Supporting Information

Stretchable and biodegradable plant-based redox-diffusion battery

Aiman Rahmanudin,*[a,b] Mohsen Mohammadi,[a,b] Patrik Isacsson, [a,b,c] Yuyang Li,[a] Laura Seufert,[a] Nara Kim,[a] Saeed Mardi,[a] Isak Engquist,[a,b] Reverant Crispin,[a,b] Klas Tybrandt*[a,b]

[a]Laboratory of Organic Electronics, Department of Science and Technology, Linköping University, 602 21 Norrköping, Sweden.

[b]Wallenberg Wood Science Center, ITN, Linköping University, Norrköping, Sweden.

[c]Ahlstrom Group Innovation, 38140 Apprieu, France

* Email: aiman.rahmanudin@liu.se; klas.tybrandt@liu.se

Experimental materials and methods

Materials: The components for the paper current collector, i.e., the suspension of nanographite (NG) and unbleached kraft pulp of electrotechnical grade, was kindly provided by 2Dfab and by Ahlstrom Sweden AB, respectively. Nanostructured graphite used in the adhesion layer was purchased from Graphene Supermarket. Carboxylated Cellulose Nanofibrils (CNFs) (1wt%, degree of substitution of 0.1 ± 0.05) was prepared by Innventia AB. Lignosulfonate (average M_w 21k, 7% of sulfonic acid group) supplied by Domsjö. PEDOT:PSS (Clevios™ PH1000, 1.1–1.3 wt% aqueous dispersion) were purchased from Heraeus. Elastomers, ALBERDINGK®U4101, 39–41 wt% aqueous anionic dispersion of aliphatic polyether-polyurethane (PU) and TUFTEC™ H1052 styrene-ethylene-butylene-styrene (SEBS), was obtained from Alberdingk Boley and Asahi Kasei, respectively. Alizarin Red S (ARS), poly(styrene sulfonic acid) (PSS, average M_w 75k), Nafion117™, polyvinyl alcohol (PVA, average M_w 130k, 99+% hydrolyzed), (3-Glycidyloxypropyl)trimethoxysilane (GOPS), phosphate buffered saline (PBS) tablets, absolute ethanol (99.5%), 2-propanol, were purchased from Sigma-Aldrich. All chemicals were used as received without further purification.

Synthesis of PGS elastomer: 0.1 mol of glycerol and 0.1 mol of sebacic acid was stirred at 120°C under nitrogen for 24 h to form the pre-polymer. The viscous liquid was then poured into a teflon mold and left under pressure at 400 mbar 24 h at 70°C for degassing. The reaction mixture was then heated at 120 °C for a further 48 h to obtain the elastomer substrate.

Stretchable kirigami patterned current collector preparation: The preparation of the nanographite-filled paper current collector was adapted from previously reported procedures[1, 2] and modified to increase density, conductivity, and stretchability. The prepared papers were further processed by calendaring with 2 passes in a Durston 80 mm rolling mill. The calendared papers had a thickness of 47µm and obtained a sheet resistance of 1.01.4 ± 0.3 Ω $\square^{-1}$. A rectangular sheet (L x W - 25 x 10 mm) of NG paper was placed on a the PGS elastomer with applied pressure to ensure adhesion. MetaQuip laser was then used to form the Kirigami pattern via laser ablation at the respective slit lengths (0.5, 1.25, 1.5, 1.75, 2 mm) with the spacing lines kept at Y = 0.5 mm and x = 0.75 mm. The laser operates at a wavelength of 355 nm, a pulse repetition rate of 30 kHz, and a pulse width with of 35 ns. The focused beam spot width is approximately 20 µm so the ablated spot diameter falls under 20 µm. The control parameters repetitions, current power percent, and scanning speed are carefully adjusted to ablate the desired patterns on the current collector.

Stretchable ion-selective membrane preparation: The stretchable ion-selective membrane was prepared by mixing PU:CNF:PSS homogenized using a T10 basic ULTRA-TURRAX (Laboratory Mixers) for 3 minutes. The wt.% of WPU was kept the same while the amount of CNF:PSS were optimized. After homogenization, the slurry was centrifuged for 5 mins at 1000 rpm for degassing. The solution was then drop casted over a glass substrate containing a SEBS mold and left to dry at room temperature overnight to obtain free-standing composite films of 30 x 30 mm. The membranes were then cut to the desired shape of 15 x 15 mm and soaked in 1M H_2SO_4 for 12 hrs then placed in between to SEBS gasket containing a hole with 10 mm diameter. Before lamination, the gaskets were slightly swelled with a small amount of toluene using a cleanroom swab before placing the membrane in between the gaskets, and pressure was applied to ensure adhesion of the layers. This was then placed in a H-Cell for characterization and laminated on the half-cells for battery assembly. The same preparation method was used to measure the mechanical properties of the membranes.

Stretchable active electrode preparation: The (PEDOT:PSS):CNF:GOPS aerogel synthesis was adapted from a previously reported method.[3] These three components were mixed at a wt. ratio of 1:1:0.5 using a T10 basic ULTRA-TURRAX. The volume of water:ethanol (H_2O:EtOH) content was varied from 1:0, 9:1, 4:1, and 7:3. The solution was then centrifuged at 2000 rpm for 3 mins for degassing. A fixed volume of 30 µL was pipette into SEBS mold with a diameter of 8 mm and thickness of 0.5 mm to ensure consistency of the shape, size, and mass loading of the aerogel. This was then frozen using liquid nitrogen

followed by freeze drying (Benchtop Pro, SP SCIENTIFIC) under −60 °C and 50 µbar for 12 h. The aerogels were then placed into an oven at 140 °C for 1hr initiate the crosslinking reaction between GOPS, PEDOT:PSS and CNF. The synthesized aerogels had a density of 8.45 mg/cm^3. For the adhesion of the aerogel to the current collector, GNP:PU adhesion solution were prepared by shear mixing a solution of NG in IPA (16 mg/mL) and PU in DI H_2O (16 mg/mL) at a volume ratio of 1:1 using a T10 basic ULTRA-TURRAX for 3 mins. 25 µL of the adhesion solution was then dropped onto the 10 mm diameter area of the current collector and the solvent was left to partially dry for about 2 mins before adding another 25 µL. The aerogel was then carefully placed over the remaining liquid to allow absorption of the adhesion solution and left to dry at room temperature for at least 30 mins before the next step.

Redox-hydrogel electrolyte preparation: Firstly, PVA was dissolved in 1M H_2SO_4 at 50 and 5 mg/mL at 85°C for 2 h until a homogeneous and clear solution was formed. ARS and LS were weight out at the desired molar concentration in separate vial and the PVA-H_2SO_4 solution (50 mg/mL for ARS and 5 mg/mL for LS) was added and left to stir at 85°C for 1h to ensure complete dissolution of the components before infiltrating into the aerogel with 50 µL of the redox electrolyte solution.

Half- and full-cell assembly: After infiltration, the half-cell was placed in a fridge at -20 °C for 12 hrs before thawing at room temperature for 4 hrs to generate the hydrogel in the active electrode. The membrane was then placed over the active electrode using the same lamination procedure for the SEBS gaskets. The half-cells were then placed in a beaker containing 40 mL of 1M H_2SO_4 with the counter and reference electrode for electrochemical characterization. For the full cell, the membrane was placed over a half-cell without the SEBS gaskets with the other half-cell stacked in a sandwich structure using applied pressure according to a previously reported procedure.[4]

Degradation Experiment: PGS samples were immersed in a PBS solution at various temperatures (25 °C, 37 °C and 85 °C) over a period of 8 weeks. The mass of the samples was taken every 7 days. The samples were rinsed with DI water and dried before measuring its weight and the PBS solution was replaced before continuing with the degradation. For the full cell, the sample was placed in a beaker and immersed in PBS at 85 °C.

Characterization

Mechanical and electrical, characterization: The electromechanical analysis of the current collector was performed by clamping the respective free-standing films on a motorized linear stage (X-LSQ300A-E01, Zaber) with gold-coated 4-point contact pads connected to a Keithley 2701 Ethernet Multimeter data acquisition system for the resistance vs. strain measurements. The mechanical properties (stress vs. strain) of the respective materials was analysed using a force gauge meter (M5-2, Mark-10) attached with a motorized linear stage as described above. For all measurements, a strain rate (mm/s) of 1% of the length of the sample which was 10 mm, was used for the maximum resistance and elongation tests, and a strain rate of 2% was used for the cycling tests.

XRD: X-ray powder diffraction patterns are characterized by X'Pert Pro (PANalytical, The Netherlands) diffractometer with monochromatic Cu-Kα1 radiation (λ= 1.5406 Å) at 40 kV and 40 mA. The diffraction patterns are optimized with a step length of 0.01° (2θ) over an angular range 10–60° (2θ) with a scanning speed of 0.01° s-1.

Dynamic light Scattering: The hydrodynamic sizes and polydispersity of PU:CNF:PSS emulsions samples are characterized by Zetasizer Nano ZS90 (Malvern, UK). PU:CNF:PSS emulsions is diluted and dispersed in DI water within polystyrene cuvette, the detector collected the scattered light at 90° direction to the laser.

Optical absorption and transmittance spectroscopy: The optical and absorption spectra were measured using a UV–vis–NIR spectrometer (Lambda 900 (Perkin Elmer Instruments)) in the range from 250 to 600 nm.

Electrochemical characterization: All electrochemical measurements (CV, GCD and EIS) were performed using a Gamry 1001E potentiostat. The ionic conductivity of the membrane in its initial and stretched state was obtained by measuring the impedance using a four-point method across the electrolyte with and without the membrane in a H-Cell set-up (See Fig S1.). For the membrane conductivity, the impedance was measured across a frequency range of 0.1 to 10k Hz with an AC voltage of 10 mV using two reference electrodes (Ag/AgCl in 3M KCl) to detect the local potential drop and two coiled platinum wire electrodes to apply the AC current. Ionic conductivity was deduced from the measured impedance of the system with (R_s) and without (R_0) the membrane using following formula: $s = h / (R_s - R_0) A$, where h and A are the thickness and the area of the separator. The hydrogel conductivity was extracted by measuring the impedance of the hydrogel across a frequency range of 0.1 to 10k Hz with an AC voltage of 10 mV with the hydrogel sandwiched between 2-electrodes (Au/Cr on glass). The impedance was extracted at high frequencies region that correlates to the resistive regime (phase angle = 0^0) and the conductivity (s) was calculated from the formula $s= t/AR$, where t is the thickness and A is the area of the electrode, and R is the measured impedance. All half-cells were measured using a three-electrode configuration with a coiled Pt wire as the counter electrode, Ag/AgCl electrode as the reference electrode and 1M H_2SO_4 as the electrolyte that was purged with N_2 gas to remove oxygen before conducting the relevant CV and GCD tests. The charge storage kinetics of the cathodes and anodes were established from the b values (0.5-1) that were estimated from fitting the curve based on the equation $\text{Log}(i) = b \times \text{Log}(v) + \text{Log}(a)$, where the peak current, i (A/cm^2) and scan rate v (mV/s) were extracted from the respective CV plots of the half-

cells. For discharge and impedance measurements in stretched states, the battery was clamped on to a motorized linear stage (X-LSQ300A-E01, Zaber) connected to a Gamry 1001E potentiostat.

Statistical analysis

Sample size for all experiments were n = 3 per type (current collector, membranes, half- and full cells). Data points being mean values and error bars indicating standard deviation. All measurement data are plotted as recorded.

Table S1. Comparison of relevant state-of-the-art electrochemical energy storage (EES) system

Battery Design	Sustainable Material Selection[a]	Degradable	Battery Type	Voltage [V]	Capacity	Mechanical Properties	Ref
Plant-based							
Active Electrode – Plant-based (Alizarin and Lignin) – PEDOT:PSS – Mass ratio of CF:RA (285:1) **Electrolyte** – Hydrogel PVA in 1M H_2SO_4. **Separator membrane** – CNF and PU **Current Collector** – Cellulose and nanographite **Encapsulation** – Biomass-derived PGS Elastomer	Yes	Yes	Secondary	0.6	Full cell-2.68 $mAhcm^{-3}$ at 0.2 $mAcm^{-2}$ For Anode, Gravimetric capacity is 121.1 mAh/g at 1 $mAcm^{-2}$	Stretchable up to 30 % strain	This work*
Active Electrode – Plant-based Ligninsulfonate – PEDOT:PSS:CNF – CF:RA , 1:2 **Electrolyte** – 0.1M $HClO_4$. **Current Collector** – Carbon fiber **Encapsulation** – Glass	Partial (Only LS aand CNF)	No	Supercapacitor, Half-cell	0.6	230 F g^{-1}, 1 F cm^{-2}.	No mechanical characterisation	5
Active Electrode – Plant-based Lignin – PEDOT – CF:RA , 3:2 **Electrolyte** – 0.1M $HClO_4$. **Current Collector** – Carbon fiber **Encapsulation** Glass	Partial (Only LS)	No	Supercapacitor, Half-cell	0.6	Half-cell, PEDOT:Lignin (3:2), 115.0 F g^{-1}, 28.0 $mAhg^{-1}$ PEDOT:lignin (Electrodeposited 600s), 170.4 F g^{-1}, 34.1 $mAhg^{-1}$	No mechanical characterisation	6
Active Electrode – Plant-based Kraft Lignin – Carbon Black – CF:RA , 1:1 **Electrolyte** – 0.1M $HClO_4$. **Current Collector** – Stainless steel	Partial (Only LS)	No	Battery Hal-cell	0.6	49 $mAhg^{-1}$ at 0.25 Ag^{-1}	No mechanical characterisation	7

Active Electrode – Plant-based Juglone redox biomolecules. **Electrolyte** – Hydrogel PVA in 1M H_2SO_4. **Current Collector** – Carbon cloth and Au Film **Encapsulation** – PET	Partial (only redox molecule)	No	Supercapacitor	0.8	45.1 $mFcm^{-2}$ and 56.3 Fg^{-1} at 1 $mAcm^{-2}$	Flexible	8
Active Electrode – Plant-based Alizarin Red S – PEDOT:PSS:CNF – CF:RA , 1:10 **Electrolyte** – Hydrogel 0.1M $HClO_4$. **Current Collector** – Carbon and Au Film **Encapsulation - g**lass	Partial (only redox molecule and CNF binder)	No	Supercapacitor	1.2 V	400 F g^{-1},	No mechanical characterisation	9
Active Electrode – Plant-based Alizarin redox biomolecule and Methylene blue **Electrolyte** – Hydrogel PVA in 1M H_2SO_4. **Current Collector** – Carbon Fiber **Encapsulation** PET	Partial (only redox molecule)	No	Supercapacitor	1.0	Length capacitance of up to 12.7 and 8.7 mF cm^{-1},	Flexible	10
Active Electrode – Plant-based Alizarin redox biomolecule. **Electrolyte** – Hydrogel PVA in 1M H_2SO_4. **Current Collector** – Stainless steel net and Activated carbon **Encapsulation** – N/A	Partial (only redox molecule)	No	Supercapacitor	1.0	441 F g^{-1} at 0.5 Ag^{-1}	Flexible	11
Active Electrode – Cathode: Bis(3-trimethylammonio) propyl viologen tetrachloride (BTMAP-Vi) – Anode: bis((3-trimethylammonio)propyl)ferrocene (BTMAP-Fc) **Electrolyte** – Hydrogel Agarose in KCl. **Separator membrane** – Selemion DSV anion exchange membrane **Current Collector** – Carbon Fiber **Encapsulation** – Silicone Resin	Partial (only polymer used for hydrogel electrolyte)	No	Battery[c]	0.75	0.39 mA h cm^{-2} μm^{-1}	No mechanical characterisation	12
Active Electrode – Cathode: hydroquinone (Anode) and methylene blue (Cathode) **Electrolyte** – Hydrogel PVA in 1M H_2SO_4. **Separator membrane** – Nafion **Current Collector** – Carbon Fiber **Encapsulation**	No	No	Supercapacitor[c]	1.0	563.7 F g^{-1}	No mechanical characterisation	13

– Silicone Resin							
Stretchable and Biodegradable Batteries							
Active Electrode • Mo-Mg (Primary) **Electrolyte** • Gelatin and Citric Acid **Current Collector** • Mo and Mg **Encapsulation** • Paper substrate (Cellulose)	Partial [b]	Yes	Primary	1.4	2.9 μAh cm^{-2} at 40 μA cm^{-2}	Stretchable up to 30 % strain	14
Active Electrode • Mg-MoO3 (Primary) **Electrolyte** • Hydrogel Alginate and $CaCl_2$ **Current Collector** • Mg and Mo Metal **Encapsulation** • Biomass-derived PGS Elastomer	Partial [b]	Yes	Primary	1.73	4.7 mAh at 45 μA cm^{-2}	Flexible & Stretchable up to 35 % strain	4
Stretchable Organic Batteries							
Active Electrode • Redox-active polymers, poly(TEMPO- substituted acrylamide) (PTAm) and poly(anthraquinone-. Substituted ethyleneimine) (PAQE), as the cathode- and anode-active polymers, (Secondary) **Electrolyte** • Poly(ethylene glycol) hydrogel in NaCl (aq) **Current Collector** • SWNT **Encapsulation** Poly(styrene–buta-diene–styrene)	No. Mostly. Petrochemical -based	No	Secondary	1.2	60 $mAhg^{-1}$ at 18 C	stretchable up to 40 % strain	15
Active Electrode • Redox-active molecules Alizarin • Mass ratio of ARS/PEDOT (4:1) **Electrolyte** – Hydrogel PVA in 1M H_3PO_4. **Current Collector** • Au Nanowires **Encapsulation** SEBS	Mostly petrochemical -based, only the redox-molecule is plant based.	No	Secondary	0.8	44 μAh cm^{-2} at 0.5 mA cm^{-2}	stretchable up to 120 % strain	16

[a] Sustainability is defined as materials derived from renewable biomass feedstocks as discussed in the introduction of the main text.[17]
[b] As discussed in the introduction in the main text, degradable metals are highly abundant but they are still a finite resource, and the ethical, social and environmental concerns of mining and the energy intensive processing are still problematic.[18, 19]
[c] Based on dissolved redox-active molecules in the electrolyte.

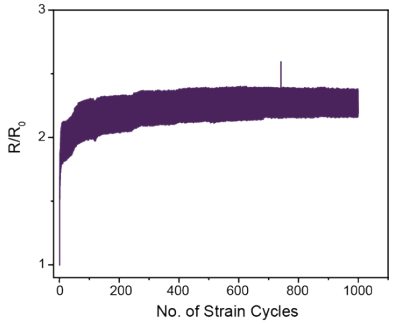

Fig S1. Cyclic stretching of the kirigami current collector at 150 % strain over 1000 cycles.

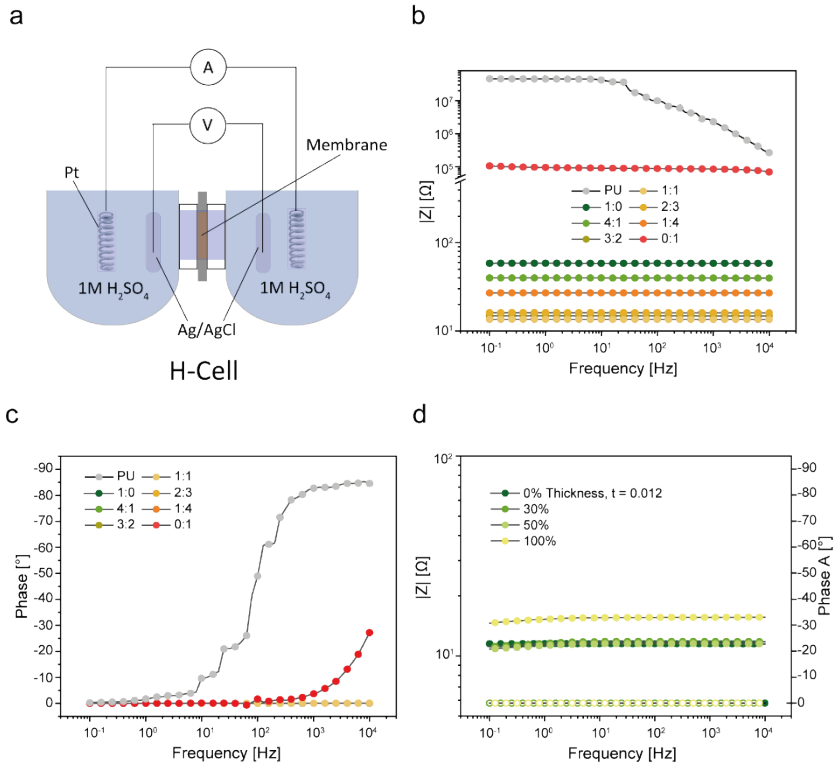

Fig. S2. EIS characterization of the ion-selective membranes. a) Schematic of the four-point H-Cell set-up; Bode plots of the membranes: b and c.) as a function of CNF:PSS ratio, and d) at the various stretch states.

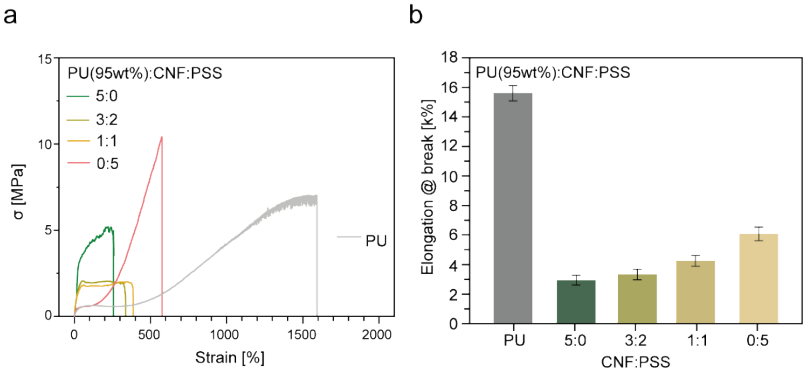

Fig. S3. Mechanical properties of the PU:CNF:PSS membranes after soaking in 1M H_2SO_4 for 24 h a) stress-strain curves used to extract the young's modulus and the b) their elongation at break.

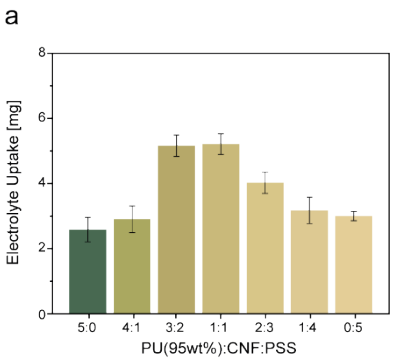

Fig. S4. a) Membrane electrolyte uptake as: as a function of CNF:PSS ratio.

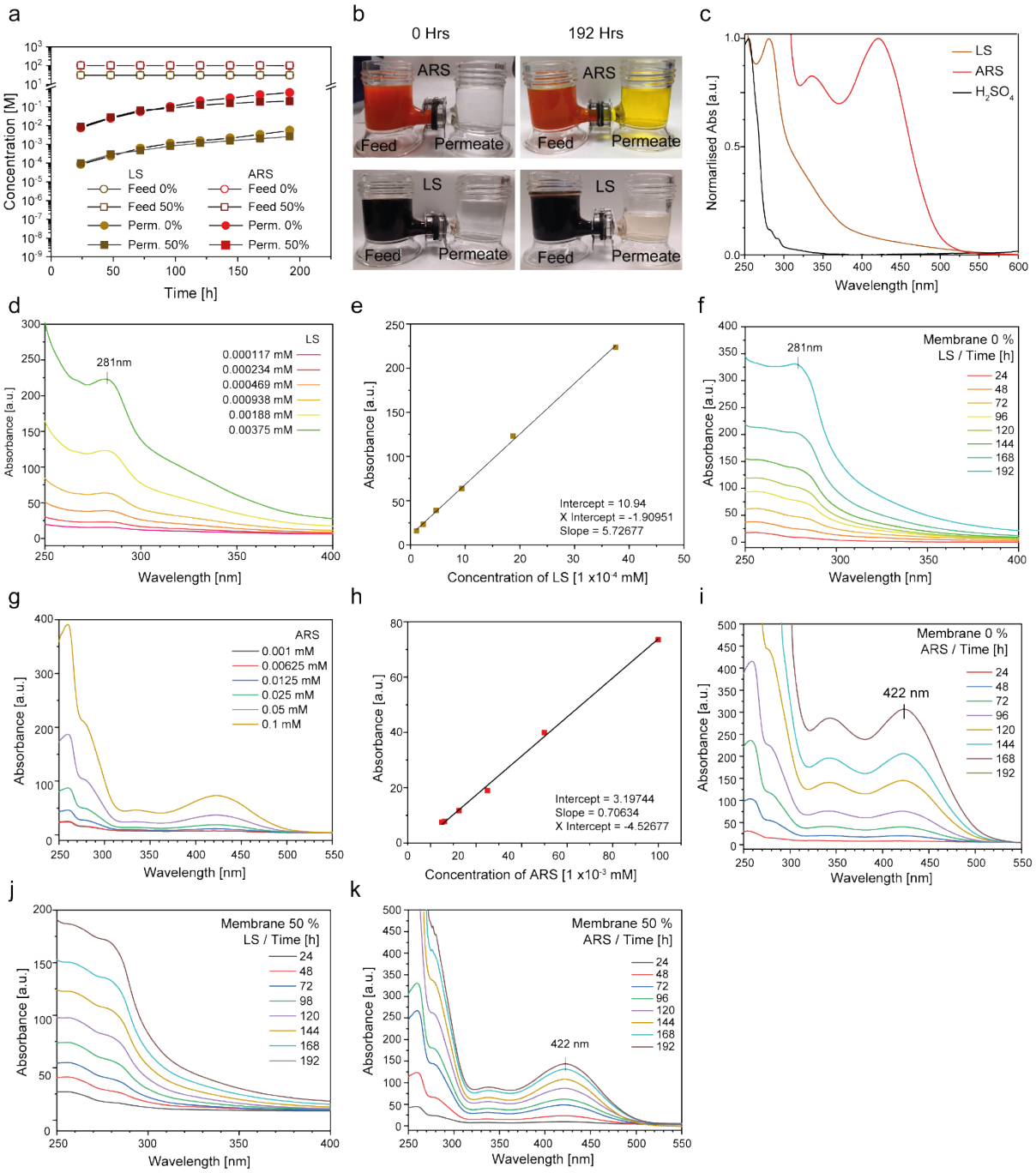

Fig. S5. Membrane cross-over characterisation. a) Plot of the concentration of the feed and permeate of ARS and LS as function of time for membrane in its initial state 0 % and 50 % strain. b) Representative digital photographs of the H-cell before and after 192 h. c) Normalised optical absorption spectra of ARS and LS dissolved in 1M H_2SO_4. d) Absorption of LS at various concentrations; e) Concentration calibration curves for LS. f) Absorption spectra of LS permeate taken at various time intervals for membranes at 0 % strain. g) Absorption of ARS at various concentrations; h) Concentration calibration curves for ARS. i) Absorption spectra of ARS permeate taken at various time intervals for membrane at 0 % strain. j.) Absorption spectra of LS permeate taken at various time intervals for membrane at 50 % strain. k.) Absorption spectra of ARS permeate taken at various time intervals for membrane at 50 % strain.

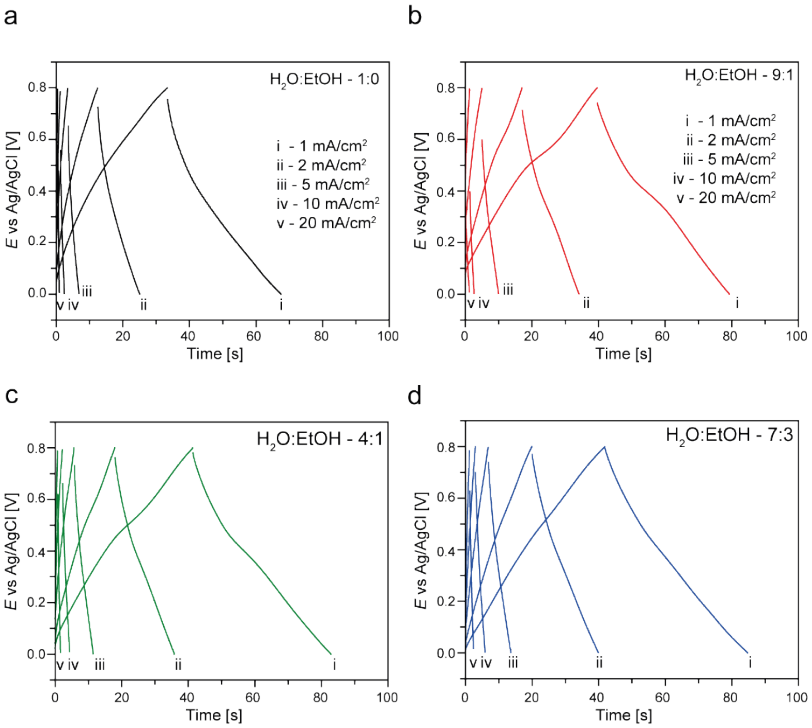

Fig. S6. GCD curves of the aerogel prepared at various H_20:EtOH ratios: a) 1:0, b) 9:1, c) 4:1, d) 7:3.

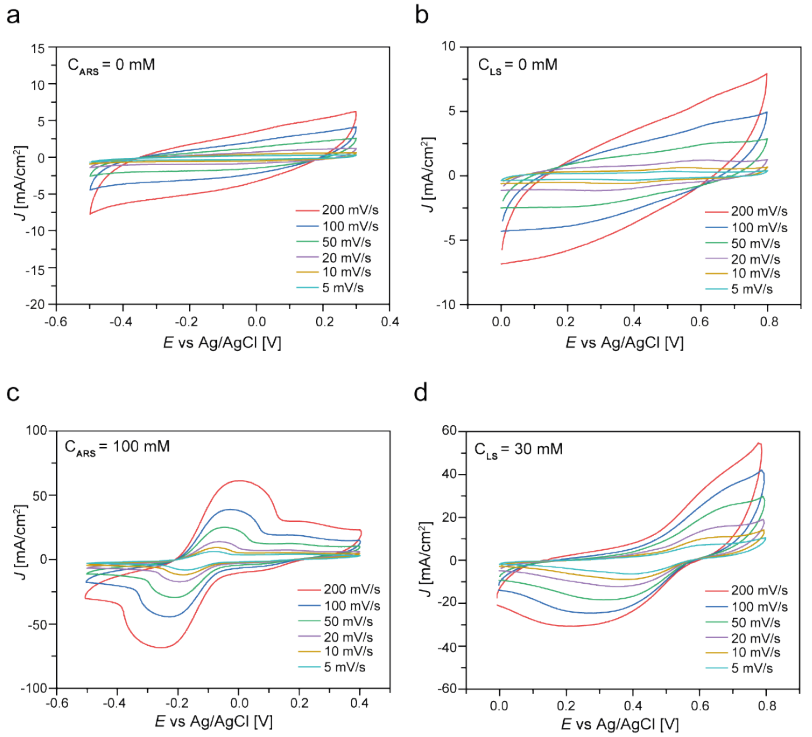

Fig. S7. CV curves of the half-cells at various scan rates: a) C_{ARS} = 0 mM, b) C_{LS} = 0 mM, c) C_{ARS} = 100 mM, d) b) C_{LS} = 30 mM.

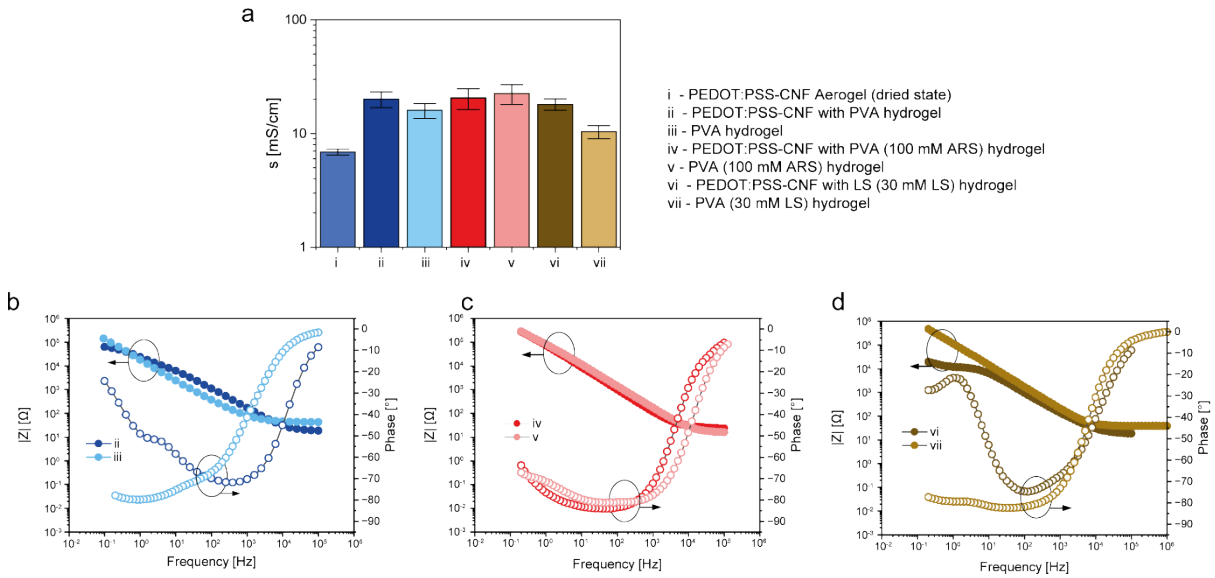

Fig. S8. a) Conductivity of the respective hydrogel electrodes including the PEDOT:PSS-CNF aerogel scaffold in the dried state (i). Bode plots of EIS measurements of the electrodes for b) PVA (1M H_2SO_4) with (ii) and without (iii) the PEDOT:PSS-CNF scaffold. c) PVA (1M H_2SO_4) with dissolved ARS (100 mM) with (iv) and without (v) the PEDOT:PSS-CNF scaffold. d) c) PVA (1M H_2SO_4) with dissolved LS (30 mM) with (vi) and without (vii) the PEDOT:PSS-CNF scaffold.

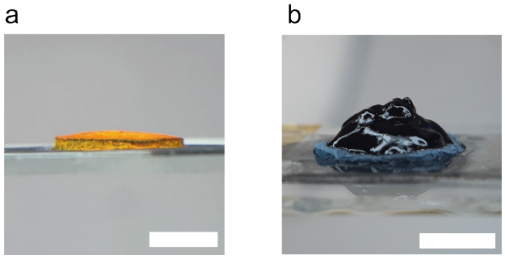

Fig. S9. Photographs of soaked aerogel with electrolytes containing a) 50 mg/mL of PVA with 100 mM of ARS in H_2SO_4 , and b) a 50 mg/mL of PVA with 30 mM of LS in H_2SO_4.

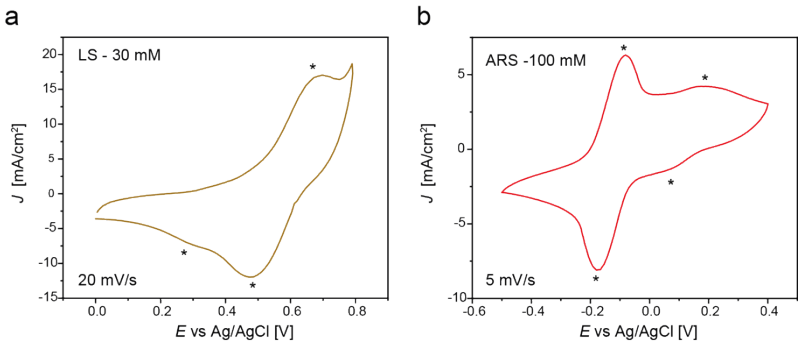

Fig S10. CV curves of a) LS and b) ARS at lower scan rates of 20 and 5 mV/s respectively. (*) denotes the redox peaks observed on the voltammograms.

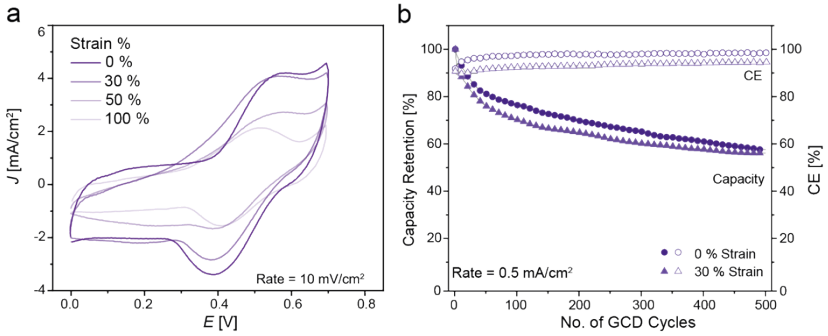

Fig S11. a) CV curves of the full cell under various stretching strains. b) Capacity retention and coulombic efficiency vs the number of GCD cycles of the full cell at 0 % and 30 % strain. The data for the full cell at 0% strain was added from Figure 6c.

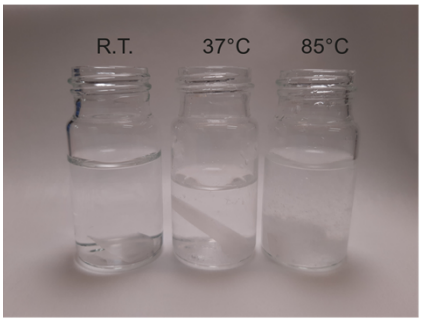

Fig. S12. Photographs of PGS samples in PBS after soaking a) 50 mg/mL of PVA with 100 mM of ARS in H_2SO_4 , and b) a 50 mg/mL of PVA with 30 mM of LS in H_2SO_4.

Table S2. Biodegradation characteristics of the battery components

Materials	Degradability	Pathway	Products	Ref
Encapsulation	Type II			
PGS	F	70 d, Hydrolysis via de-esterification	Glycerol, sebacic acid	20
Current collector	Type II			
CF	F	Enzymatic	Glucose	21
Graphite	F	non-toxic, enzymatic	-	22
Cathode/Anode	Type II			
CNF	F	Enzymatic, 60 d	Glucose	21
LS	F	Enzymatic	Low M_w Lignin chains	
ARS	F	Photocatalytic or enzymatic	Phenolic and carboxylic acid compounds	23, 24
PVA	F	Enzymatic, hydrolysis, oxidation of alcohol linkages	Low M_w PVA chains	25, 26
PEDOT:PSS	F	Microorganism	Low M_w by-products	27
Membrane	Type I			
PU[a]	P	Hydrolysis of urethane linkages	Biomass derived Low M_w polymer chains	[7]

[a] PU is made from renewable raw materials based on castor and linseed oil.

References

1. N. Blomquist, A.-C. Engström, M. Hummelgård, B. Andres, S. Forsberg and H. Olin, 2016, **11**, e0154686.
2. P. Isacsson, X. Wang, A. Fall, D. Mengistie, E. Calvie, H. Granberg, G. Gustafsson, M. Berggren and I. Engquist, *ACS Applied Materials & Interfaces*, 2020, **12**, 48828-48835.
3. S. Han, F. Jiao, Z. U. Khan, J. Edberg, S. Fabiano and X. Crispin, *Advanced Functional Materials*, 2017, **27**, 1703549.
4. M. Karami-Mosammam, D. Danninger, D. Schiller and M. Kaltenbrunner, *Advanced Materials*, 2022, DOI: 10.1002/adma.202204457, 2204457.
5. J. Edberg, O. Inganäs, I. Engquist and M. Berggren, *Journal of Materials Chemistry A*, 2018, **6**, 145-152.
6. F. N. Ajjan, N. Casado, T. Rębiś, A. Elfwing, N. Solin, D. Mecerreyes and O. Inganäs, *Journal of Materials Chemistry A*, 2016, **4**, 1838-1847.
7. U. Ail, J. Nilsson, M. Jansson, I. A. Buyanova, Z. Wu, E. Björk, M. Berggren and X. Crispin, *Advanced Sustainable Systems*, 2023, **7**, 2200396.
8. J. Wu, D. Yu, G. Wang, J. Yang, H. Wang, X. Liu, L. Guo and X. Han, *ChemPlusChem*, 2018, **83**, 423-430.
9. J. Edberg, R. Brooke, H. Granberg, I. Engquist and M. Berggren, *Advanced Sustainable Systems*, 2019, **3**, 1900050.
10. J. Yang, H. Wang, Y. Yang, J. Wu, P. Hu and L. Guo, *Nanoscale*, 2017, **9**, 9879-9885.
11. K. Sun, F. Ran, G. Zhao, Y. Zhu, Y. Zheng, M. Ma, X. Zheng, G. Ma and Z. Lei, *RSC Advances*, 2016, **6**, 55225-55232.
12. F. N. Crespilho, G. C. Sedenho, D. De Porcellinis, E. Kerr, S. Granados-Focil, R. G. Gordon and M. J. Aziz, *Journal of Materials Chemistry A*, 2019, **7**, 24784-24787.
13. J. Zhong, L.-Q. Fan, X. Wu, J.-H. Wu, G.-J. Liu, J.-M. Lin, M.-L. Huang and Y.-L. Wei, *Electrochimica Acta*, 2015, **166**, 150-156.
14. Z. Wang, X. Li, Z. Yang, H. Guo, Y. J. Tan, G. J. Susanto, W. Cheng, W. Yang and B. C. K. Tee, *EcoMat*, 2021, **3**.
15. K. Hatakeyama-Sato, H. Wakamatsu, K. Yamagishi, T. Fujie, S. Takeoka, K. Oyaizu and H. Nishide, *Small*, 2019, **15**, 1805296.
16. N. Kim, S. Lienemann, Z. Khan, G. Greczynski, A. Rahmanudin, M. Vagin, F. Ahmed, I. Petsagkourakis, J. Edberg, X. Crispin and K. Tybrandt, *Journal of Materials Chemistry A*, 2023, **11**, 25703-25714.
17. A. Rahmanudin, Z. Khan, K. Tybrandt and N. Kim, *Journal of Materials Chemistry A*, 2023, DOI: 10.1039/d3ta03482h.
18. É. Lèbre, M. Stringer, K. Svobodova, J. R. Owen, D. Kemp, C. Côte, A. Arratia-Solar and R. K. Valenta, *Nature Communications*, 2020, **11**.
19. F. P. Carvalho, *Food and Energy Security*, 2017, **6**, 61-77.
20. M. Held, A. Pichler, J. Chabeda, N. Lam, P. Hindenberg, C. Romero-Nieto and G. Hernandez-Sosa, *Advanced Sustainable Systems*, 2022, **6**, 2100035.
21. N. B. Erdal and M. Hakkarainen, *Biomacromolecules*, 2022, **23**, 2713-2729.
22. R. Kurapati, S. P. Mukherjee, C. Martín, G. Bepete, E. Vázquez, A. Pénicaud, B. Fadeel and A. Bianco, *Angewandte Chemie International Edition*, 2018, **57**, 11722-11727.
23. L. A. Adnan, P. Sathishkumar, A. R. M. Yusoff, T. Hadibarata and F. Ameen, *Bioprocess and Biosystems Engineering*, 2017, **40**, 85-97.
24. S. K. Kansal, R. Lamba, S. K. Mehta and A. Umar, *Materials Letters*, 2013, **106**, 385-389.

25. G. Ghosh, A. Bag, A. Hanif, M. Meeseepong, Y. R. Lee and N. E. Lee, *Advanced Functional Materials*, 2022, DOI: 10.1002/adfm.202209277, 2209277.
26. N. Ben Halima, *RSC Advances*, 2016, **6**, 39823-39832.
27. S. Lee, Y. Hong and B. S. Shim, *Advanced Sustainable Systems*, 2022, **6**, 2100056.